Engineering Geology 217 (2017) 71–80

Contents lists available at ScienceDirect

Engineering Geology

journal homepage: www.elsevier.com/locate/enggeo

Interactions between groundwater and the cavity of an old slate mine used as lower reservoir of an UPSH (Underground Pumped Storage Hydroelectricity): A modelling approach

Sarah Bodeux *, Estanislao Pujades, Philippe Orban, Serge Brouyère, Alain Dassargues

University of Liege, Hydrogeology & Environmental Geology, Aquapole, ArGEnCo Dpt, B52, 4000 Liege, Belgium

ARTICLE INFO

Article history:
Received 13 May 2016
Received in revised form 14 December 2016
Accepted 16 December 2016
Available online 21 December 2016

Keywords:
Underground Pumped Storage Hydroelectricity (UPSH)
Energy storage
Groundwater modelling
Impacts
Cyclic solicitations

ABSTRACT

In the actual evolving energy context, characterized by an increasing part of intermittent renewable sources, the development of energy storage technologies are required, such as pumped storage hydroelectricity (PSH). While new sites for conventional PSH plants are getting scarce, it is proposed to use abandoned underground mines as lower reservoirs for Underground Pumped Storage Hydroelectricity (UPSH). However, the hydrogeological consequences produced by the cyclic solicitations (continuous pumpings and injections) have been poorly investigated. Therefore, in this work, groundwater interactions with the cyclically fill and empty cavity were numerically studied considering a simplified description of a slate mine. Two pumping/injection scenarios were considered, both for a reference slate rock case and for a sensitivity analysis of variations of aquifer hydraulic conductivity value. Groundwater impacts were assessed in terms of oscillations of piezometric heads and mean drawdown around the cavity. The value of the hydraulic conductivity clearly influences the magnitude of the aquifer response. Studying interactions with the cavity highlighted that seepage into the cavity occurs over time. The volume of seeped water varies depending on the hydraulic conductivity and it could become non-negligible in the UPSH operations. These preliminary results allow finally considering first geological feasibility aspects, which could vary conversely according to the hydraulic conductivity value and to the considered groundwater impacts.

1. Introduction

Access to energy resources and supply stability have become strategic elements in worldwide policy decisions. Climate change and limitations of fossil fuels reserves have brought renewable energy resources for electricity production to the limelight of global concern. It is therefore expected that renewable energy sources (RES) should triple their total installed capacity in the following three decades (IEA, 2015). However, these energy sources experience fluctuations through time, producing energy in a quite different pattern than needed by the demand. Energy storage systems are then required to deal with this intermittency as they provide flexibility by shifting the load temporally (Bussar et al., 2016; Moriarty and Honnery, 2016).

Pumped Storage Hydroelectricity (PSH) is an old and well-known mature technology for large-scale storage of electricity (Deane et al., 2010; Steffen, 2012; Yekini Suberu et al., 2014). During periods of low electricity demand, the excess of generated energy is stored by pumping water from a lower to an upper reservoir. Conversely, during peak demand or underproduction periods, water is released back to the lower reservoir through turbines to produce electricity (Rehman et al., 2015). Conventionally, both reservoirs are located at the surface but appropriate new sites are getting scarce for further developments of PSH (Ardizzon et al., 2014; Chen et al., 2009). Favorable topographic conditions are difficult to meet environmental and social issues (e.g. landscape, vegetation, wildlife, human activities, population settlement, water quality, water policy, etc.) have risen over time. However, in the increasing renewable energy framework, PHS technology appears as one of the key components for energy storage (Ardizzon et al., 2014).

It is proposed to re-use abandoned mines as lower reservoirs for Underground Pumped Storage Hydroelectricity (UPSH) systems to go beyond some of these constraints and to increase the number of potential sites (Fig. 1). The idea came out in the late 1970's (Tam et al., 1978) and has been afterwards investigated in different conditions but no facility has been yet installed. In the 1980s, Braat et al. (1985) and de Haan and Min (1984) proposed to install an UPSH in the Netherlands but the project was not implanted for reasons such as the inadequate characteristics of the soil. In Singapore, Wong (1996) pointed out the possibility of using abandoned rock quarries as upper reservoirs of UPSH plants by transforming drilled tunnels and shafts as lower reservoir. The taconite mine area in Minnesota (USA) was investigated economically and technically to select ten potential sites to develop UPSH

* Corresponding author.
E-mail address: Sarah.Bodeux@alumni.ulg.ac.be (S. Bodeux).

http://dx.doi.org/10.1016/j.enggeo.2016.12.007
0013-7952/

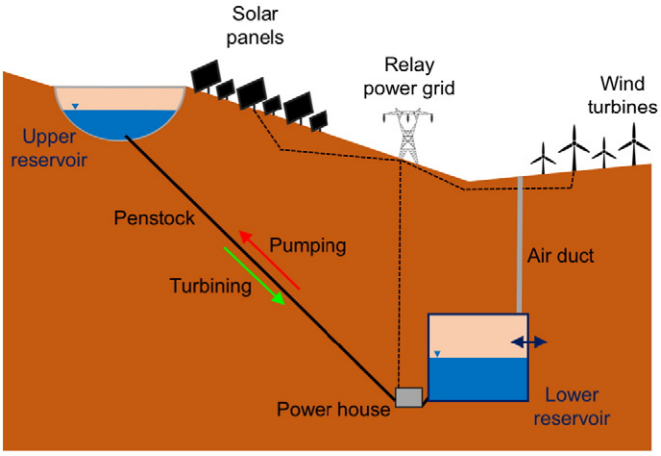

Fig. 1. Schematic representation of an Underground Pumped Storage Hydroelectricity (UPSH) plant using an old mine as lower reservoir.

plants in the non-used underground mines (Fosnacht, 2011; Martin, 2007; Severson, 2011). In Europe, the Harz and Ruhr regions in Germany have been investigated to assess the possibilities for constructing UPSH plants in abandoned coal mines (Alvarado and Niemann, 2015; Beck and Schmidt, 2011; Luick et al., 2012; Madlener and Specht, 2013; Meyer, 2013; Niemann, 2011; Steffen, 2012). In South Africa, Khan and Davidson (2016) highlighted the possibilities and the economic benefits of using existing mines and the surrounding aquifers for UPSH applications. In Belgium, recent work are studying the technical possibilities of transforming abandoned quarries (Poulain et al., 2016) or slate mines (Spriet, 2013) as reservoirs for future UPSH developments.

While UPSH appears as a solution to increase the pumped storage capacity, the re-use of abandoned underground mines brings questions about the impacts on the geological medium and, particularly, on groundwater resources. It is expected that the successive filling and emptying of the cavity, due to the pumping/injection cycles, will interact with the surrounding groundwater. It is required to investigate on how and with which magnitude the oscillations of water level in the cavity will be transmitted in the local aquifer as well as on the interactions between the aquifer and the cavity.

Almost no precise study has been carried out about this topic. Pujades et al. (2016) carried out a first parametric impact study with a simplified representative square open-pit mine. They highlight that pumping/injection in the reservoir induces piezometric head oscillations around the cavity, but the impacts vary according to the hydrogeological parameters of the aquifer, the properties of the underground reservoir, the boundary conditions, and the characteristics of pumping/injection time periods. Those results were only suitable for open pits mines where the volume of water pumped or injected is not an issue in comparison with the huge total volume of the open pit mine. The limited head variations would not create important gradients between the cavity head and the aquifer piezometric head. On the contrary, in deep mines, it is most often required to use the whole volume of the mine to obtain a system considered as economically and energetically interesting. Consequently, the head variation in the cavity could be more important. The subsequent head gradient would create groundwater inflows that could affect negatively the efficiency of the UPSH by adding water volume to be pumped or reducing the water volume that can be injected in the cavity. In addition, Pujades et al., 2016 considered a cavity that was not totally saturated. As a result, although hydraulic head recovers totally after a pumping, the pumped water could be released into the cavity. However, the slate mine considered in this study is completely located below the water table. Consequently, the amount of released water may be limited if water inflows after a pumping fill appreciably the cavity, which affects the feasibility of UPSH plants.

In the Belgian mining context, slate mines turn out to be one of the most promising type of sites for deep mine UPSH applications in terms of rock properties (permeability and rock strength). In this framework, this paper focuses on the case of an underground slate mine using numerical modelling as a tool for providing predictive results. Representative geological properties are first considered in a reference case. The main impacts on the surrounding geological medium are assessed through the computed piezometric head evolutions (magnitude and influence area) and the mean drawdown. Interactions between the cavity and the medium are highlighted and calculated through the water seepage into the cavity. In a second case, the influence of the hydraulic conductivity (K) of the surrounding geological medium on the predicted interactions for the chosen slate mine geometrical configuration is assessed. Based on the results, it is proposed to point out some specificities about the interactions between the cavity and the groundwater and about the long term behavior under cyclic stresses. These observations are finally brought together in a feasibility point of view of such underground storage.

2. Methodology

2.1. Modelling approach

Groundwater modelling in mining contexts is challenging because they correspond to mixed contexts involving porous media and large voids (Adams and Younger, 2001; Ghasemizadeh et al., 2012; Rapantová et al., 2007; Sherwood and Younger, 1994; Surinaidu et al., 2014). The Hybrid Finite Element Mixing Cell (HFEMC) method (Brouyère et al., 2009; Wildemeersch et al., 2010), implemented in the SUFT3D code (Brouyère, 2001; Brouyère et al., 2004; Carabin and Dassargues, 1999), is a flexible method combining advantages of black-box models together with physically based and spatially distributed models. The HEFMC method allows working with mixing cells corresponding to linear reservoirs and finite elements of porous medium together in the same mesh. Interactions between zones are considered thanks to internal boundary conditions (Brouyère et al., 2009; Wildemeersch et al., 2010).

A full description and verification of the HFEMC method was presented by Brouyère et al. (2009). Wildemeersch et al. (2010) used the method for a mined area in Belgium. The principle is to divide the modeled zone into several subdomains. Each subdomain can be either a reservoir represented by a mixing cell or a zone of porous medium (finite elements with spatially distributed properties). The mined zones can be modeled using linear reservoirs. Linear reservoirs are equivalent to a box model technique where each reservoir or box is characterized by a computed mean water level. Water flow in or out a reservoir is described by a transfer equation (Eq. (1)). The unmined zones are discretized with finite elements and groundwater flow equation in variably saturated porous media (Richards equation, Eq. (2)) is solved for providing the spatially distributed piezometric head in the simulated domain.

$$Q_{LR} = S_{LR} A_{LR} \frac{\partial H_{LR}}{\partial t} = -\alpha A_{exc}(H_{LR} - H) + Q \tag{1}$$

$$F \frac{\partial h}{\partial t} = \nabla\left(K_r \underline{\underline{K_s}} \nabla(h + z)\right) + q \tag{2}$$

where $Q_{LR}$is the flow rate entering or leaving the linear reservoir $[L^3T^{-1}]$, S_{LR} the storage of the linear reservoir $[-]$, A_{LR} the section of the linear reservoir $[L^2]$, H_{LR} the hydraulic head in the reservoir $[L]$, α the exchange coefficient between the linear reservoir with the external domain $[T^{-1}]$, A_{exc} the exchange area between the linear reservoir with the external domain $[L^2]$, H the piezometric head in the adjacent domain

[L], Q the source/sink term [L^3T^{-1}], F the generalized (in variably saturated conditions) specific storage coefficient of the porous medium [L^{-1}], h the pressure potential [L], K_r the relative hydraulic conductivity [LT^{-1}], K_s the saturated hydraulic conductivity [LT^{-1}], z the gravity potential [L], and q the source/sink term by unit volume [T^{-1}]. $H = h + z$ and $F = S_s + \frac{\partial\theta}{\partial h}$ where S_s is the specific storage [L^{-1}] and θ the water content given by a retention curve [−], considering water and media compressibilities only in the saturated part of the soil.

Interactions between each subdomain can be described by internal boundary conditions: Dirichlet (1st type) dynamic boundary condition when continuity of head is assumed across the boundary, Neumann (2nd type) impervious boundary condition for no flow boundaries between subdomains, and Fourier (3rd type) dynamic boundary condition to assume a flux across the interface proportional to the head difference. The term 'dynamic' is used to highlight the fact that the hydraulic heads calculated on the boundary are time-varying unknowns of the problem (i.e. they are calculated at each time-step).

2.2. Case study characteristics

Slate mines geometry may be highly complex and each particular mine is specific. If the mine has been abandoned for years, its characteristics are often badly documented. Consequently, as a first step, and based on the geometry of a potential specific site of a slate mine in the Ardennes region of Belgium, the here modeled underground cavity is simplified (Fig. 2). It is based on a typical one-chamber slate mine geometry of 50 m by 20 m on 50 m height. At the top of the cavity, a 30 m height rectangular prism, which links the underground cavity to the surface, is added to conceptually represent the well of a mine. The surrounding geological environment is extended up horizontally to 200 m away from the cavity and vertically to 50 m below the cavity and 30 m above the cavity roof. The domain is divided into 12 vertical layers of 10 m thick, except at the bottom of the domain where the thickness of two layers is set at 20 m and at the bottom of the cavity where the thickness of two layers is set at 5 m. The horizontal element size is about 45 m at the boundaries and is refined down to 8.5 m around the cavity.

The model consists in a 3D prismatic mesh. It is divided into two subdomains: a linear reservoir for the cavity and a subdomain made of finite elements of porous medium for the surrounding aquifer. An internal Fourier dynamic boundary condition is set at the interface between subdomains to simulate groundwater exchanges. It is derived from the second term of Eq. (1) (Brouyère et al., 2009; Wildemeersch et al., 2010):

$$Q_{FBC} = \alpha A_{exc}(H - H_{LR}) \tag{3}$$

where Q_{FBC} is the exchanged flow through the Fourier (3rd type) internal boundary condition [L^3T^{-1}], α the exchange coefficient between the linear reservoir with the external domain [T^{-1}], A_{exc} the exchange area between the linear reservoir with the external domain [L^2], H the piezometric head in the aquifer and H_{LR} the hydraulic head in the underground reservoir [L]. The exchange coefficient is used to simulate possible lining conditions of the mine walls: α values closed to aquifer hydraulic conductivity (or higher) mean no lined walls conditions while α values lower than aquifer hydraulic conductivity define lined walls conditions. In each simulation described here after, the α values are equal to K values to represent non-lined walls. Actually, α is numerically defined by $\alpha = K/b$, with b [L] corresponding to distance between the reservoir and the porous medium. Hence, we considered a distance of 1 m in our simulations. H_{LR} is computed in the code after each time step considering the outflows from and inflows to the linear reservoir.

Two Dirichlet external boundary conditions are adopted at two lateral sides of the model with head of 80 m and 79 m, in order to obtain an initial piezometric gradient of 1 m over the model (Fig. 2). On the other boundaries, no flow conditions are prescribed. Given the adopted Dirichlet external boundary conditions and that the modeled slate mine is located in the center of the model, the initial head inside the cavity is 79.5 m.

The values of parameters chosen for the reference case (Table 1) are typical of slate mines and were chosen to be representative of the rock properties of the potential mine site in Belgium (Bear and Cheng, 2010; DGO3, 2008). The same parameters are used for the sensitivity analysis but varying the hydraulic conductivity from 1×10^{-5} to 1×10^{-9} m/s, which are potential values depending on the fracturing (Bear and Cheng, 2010). To apprehend the sensitivity of the response, we first consider hydraulic conductivity because it is the main rock property that was expected to change in slate and, thus, that would influence the aquifer response. In addition, as α is considered representative to the hydraulic conductivity, its value was changed in parallel to the hydraulic conductivity in order to avoid any influence of the "rock-reservoir" interface conditions to the aquifer response.

The porous medium is considered as homogeneous and isotropic in all simulations because the objective of this work is to obtain general and representative results that are useful as a first approach of the interaction between groundwater and future UPSH plants. The representation of the results would have been limited if in homogeneities such as fractures would have been considered. Obviously, more detailed models will be required during the design stage of future UPSH plants. In the variably saturated porous medium, the retention curve and the related relative hydraulic conductivity are chosen as defined by Yeh (1987):

$$\theta = \theta_r + \frac{(\theta_s - \theta_r)}{h_b - h_a}(h - h_a) \tag{4}$$

$$K_r(\theta) = \frac{\theta - \theta_r}{\theta_s - \theta_r} \tag{5}$$

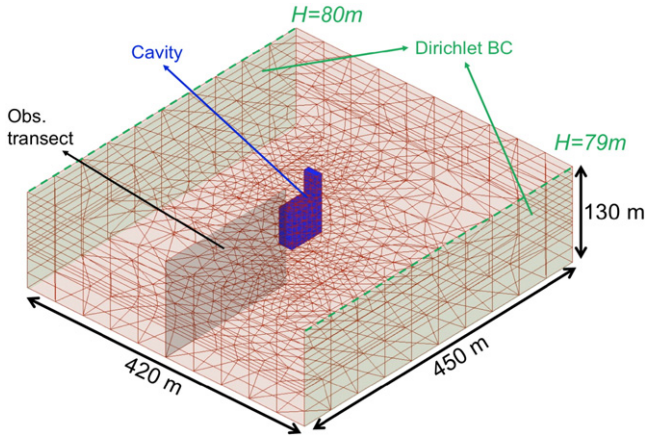

Fig. 2. General view and geometry of the numerical model. Light green surfaces represent Dirichlet external boundary conditions with corresponding piezometric head. Light grey surface represents the transect along which simulated piezometric head are observed at 75 m deep (corresponding to 55 m above the bottom of the mesh).

Table 1
Value of main parameters used in the simplified SUFT3D model for an UPSH in an old slate mine (Bear and Cheng, 2010; DGO3, 2008).

Parameters	Value	Unit
K	1×10^{-7}	m s^{-1}
S_s	1×10^{-4}	s^{-1}
θ_r	0.01	–
θ_s	0.05	–
h_b	0	m
h_a	−5	m
α	1×10^{-7}	s^{-1}

where θ_s is the saturated water content [−], θ_r the residual water content [−], h_b the pressure head for the water content of θ_s [L], h_a the pressure head for the water content of θ_r [L], and K_r the relative hydraulic conductivity [−]. Such a simple relation is considered for these first applications as studying water transfers in the unsaturated zone is clearly beyond the objectives of this paper.

The pumping and turbining cycles of the UPSH facility are represented by the pumping (or injection) of water in the saturated zone of the linear reservoir. In order to obtain a first understanding of the aquifer response, a classical day/night pattern of electricity uses has been selected. Two regular cyclic scenarios are considered (Fig. 3): scenario 1 consists of a daily cycle of 12 h of pumping and 12 h of injection; scenario 2 of a daily cycle of 8 h of pumping and 8 h of injection separated by 4 h of no-activity. These two scenarios were simulated to highlight the effect of no-activity periods. Indeed, (U)PSH are not expected to run without any no-activity periods between pumping and injection. On daily use following electricity demands, there will often be no-activity periods between high demand and low demand periods. The pumping/injection rate is constant and aims to empty/fill half the volume of the cavity (25,000 m^3) over an activity period. Consequently, it is 0.58 and 0.87 m^3/s for scenarios 1 and 2, respectively. In our model, pumping is simulated by using q in Eq. (2), which corresponds to a pumping rate applied to the cells of the linear reservoir.

Groundwater evolution is computed over a period of 84 days (≅3 months). The piezometric head evolutions are always computed at 75 m depth (corresponding to a head of 55 m) and at different distances with respect the underground cavity along a transect perpendicular to the piezometric gradient (Fig. 2).

3. Results

3.1. Reference case

Fig. 4 shows the computed head in the cavity and in the aquifer at different distances from the cavity. Fig. 4A and B show the head evolution over the whole simulation period, respectively for scenario 1 and 2. Fig. 4C and D display detailed head evolution over one week at the middle of the simulation period (day 42 to day 49). A daily mean drawdown curve at the same distance is shown in Fig. 5A. The mean drawdown is calculated based on the difference from the initial head (deduced from the initial gradient between 80 m and 79 m over the model) and the mean head per cycle (arithmetic mean of all head over 1 day). A daily water seepage volume from the surrounding aquifer into the cavity is evaluated using the daily mean hydraulic head in the cavity (Fig. 5B).

3.1.1. Piezometric response

Initially, the hydraulic head in the cavity is at equilibrium with the groundwater piezometric head. Then, the pumping of water leads to a quick decrease of the cavity hydraulic head, creating a sharp head gradient between the cavity and the aquifer (Fig. 4). In consequence, groundwater seeps into the cavity producing a decrease of piezometric head around the cavity. On the contrary, when water is injected, hydraulic head inside the cavity increases rapidly and passes above the piezometric head in the surrounding aquifer. Subsequently, water flows back from the cavity into the aquifer, increasing the surrounding piezometric head. A time lag is observed for minimum and maximum piezometric head in the surrounding aquifer with respect the minimum and maximum hydraulic heads in the cavity.

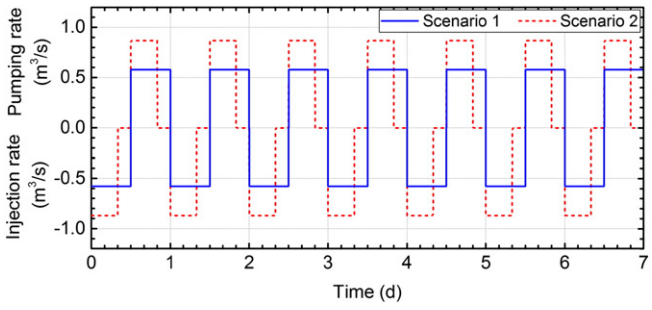

Fig. 3. Cyclic pumping/injection discharge diagrams (over 7 days) for scenario 1 without no-activity period (blue line) and for scenario 2 with no-activity periods (red dashed line). Positive discharge corresponds to pumping periods and negative discharge correspond to injection periods (turbining phase of the UPSH plant).

The repetition of water pumping and injection inside the cavity induces head oscillation in the cavity and in the surrounding aquifer (Fig. 4A & B). However, theses oscillations are damped with increasing distance from the cavity: while the oscillation magnitude still reaches few meters at 10 m, it drops near zero at a larger distance than 50 m from the cavity. In addition to the decrease of oscillation magnitude with distance from the cavity, the time lag of minimum and maximum heads between the cavity and the surrounding aquifer is also increased (Fig. 4C & D). Minimum and maximum heads in the cavity and in the surrounding aquifer display increasing values over time, reaching up to four meters at the end of the observation time. Note that the distance of the drawdown influence does not depends on the direction because the modeled porous medium is homogeneous and isotropic which is required to reach representative results.

The no-activity periods of scenario 2 are clearly visible in the head evolution in the cavity. Indeed, no-activity periods appear as head stages (Fig. 4D), slightly increasing or decreasing according that they follow pumping or injection periods. These slopes highlight the exchange of water between the cavity and the surrounding aquifer subsequently to head gradients. In the surrounding aquifer, the no-activity periods are not clearly observed. However, the no-activity periods allow the piezometric head nearby the cavity to equilibrate with the hydraulic head in the cavity: minima and maxima of oscillations are respectively lower and higher.

3.1.2. Mean drawdown

The no-activity periods of solicitation (Scenario 2) do not influence the mean drawdown in the surrounding aquifer. Indeed, mean drawdown curves of scenario 1 (Fig. 5A, solid lines) and scenario 2 (Fig. 5A, dashed lines) are superimposed. In scenario 2, the "pumping – no-activity" periods and "injection – no-activity" are identical and the total stress over one day is the same as for scenario 1. Therefore, the aquifer has the same time available to equilibrate in both scenarios. Consequently, for each pumping-injection cycle, the piezometric head oscillates around the same mean head in both scenarios. For irregular cycles or stress pattern, a strongest influence of no-activity periods would be expected.

A constant mean drawdown is reached progressively with time for both scenarios (Fig. 5A). This varies according to the distance with respect to the cavity ranging from 7 m (near the cavity) to 20 cm (at 100 m). Beyond this distance, it is reduced to almost zero at 200 m.

Beside this global trend, the dynamic of the decrease of drawdown differs according to the distance from the cavity at any stage in the operation of the UPSH. It increases gradually with a trend to stabilize at late times for further distances of 50 m. In contrast, in the surrounding aquifer closer to the cavity, the mean drawdown increases rapidly reaching a maximum value during early times and, then, it decreases progressively over time. This latter decrease is linked to the increase of both the hydraulic head inside the cavity and the piezometric levels in the surrounding aquifer (cf. Section 3.1.1). It seems that a progressive recovery of the aquifer is observed from the initial stress by equilibrating progressively the global groundwater level.

3.1.3. Water exchanges between the cavity and the surrounding aquifer

The head evolution analysis (Fig. 4) shows that the hydraulic head in the cavity increases over time. It is a result of water exchanges between

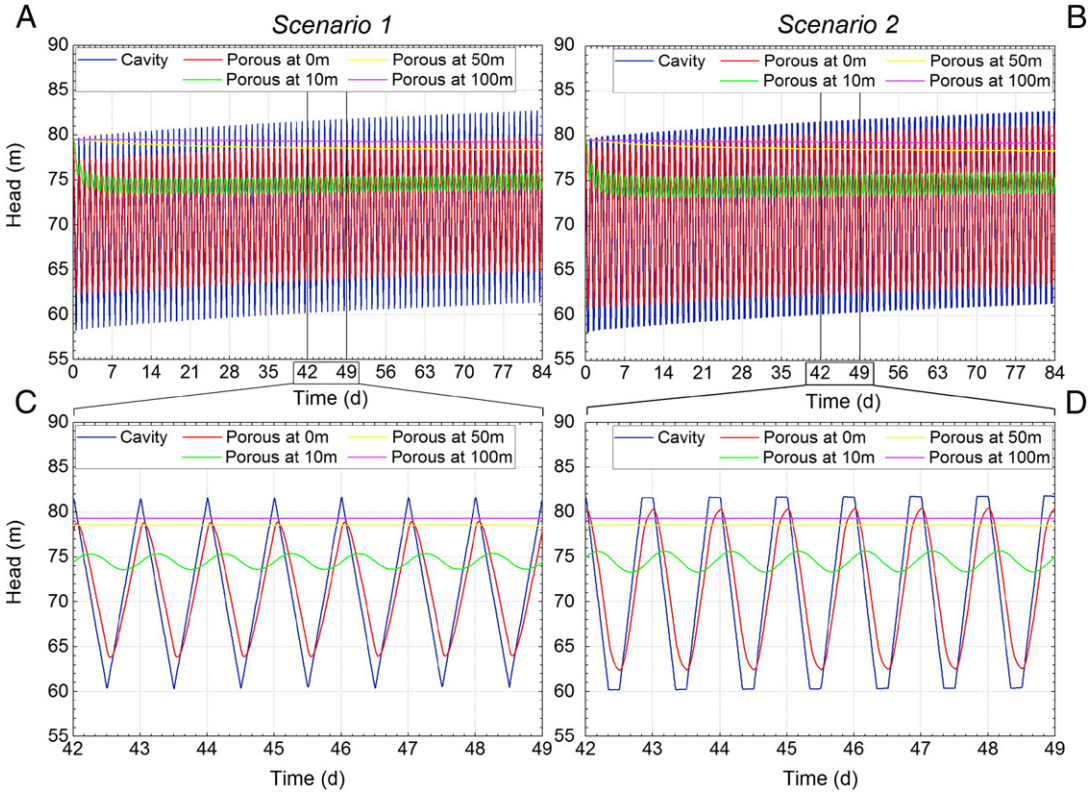

Fig. 4. Head evolution in the cavity and in the porous media at different distances from the cavity (0 m–10 m–50 m–100 m) for the reference case ($K = 1 \times 10^{-7}$ m/s). Plots A & C represent results of the scenario 1 and plots B & D represents results of the scenario 2. Plots A & B display the whole simulation times (84 days) and plots C & D detailed the head evolution between day 42 and day 49.

the cavity and the surrounding aquifer due to head gradients produced by pumping-injection cycles.

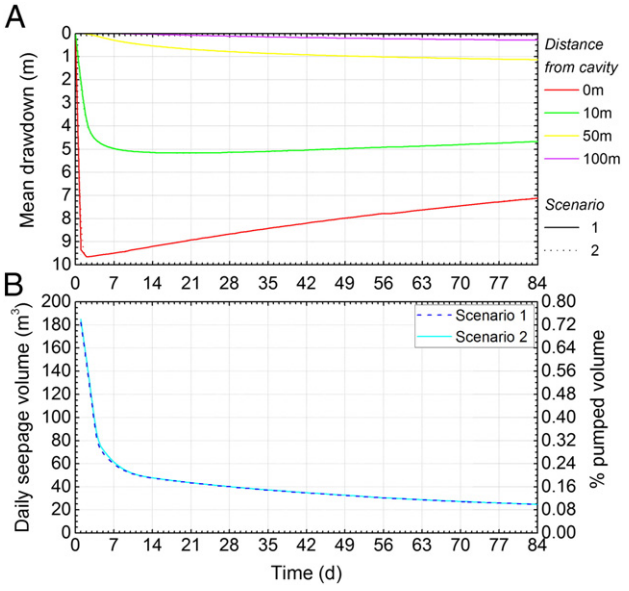

Fig. 5. A - Mean drawdown in the aquifer at different distance from the cavity (0 m–10 m–50 m–100 m) for the reference case ($K = 1 \times 10^{-7}$ m/s) with comparison of scenario 1 (solid line) and scenario 2 (dotted line). B - Daily seepage into the cavity for the reference case ($K = 1 \times 10^{-7}$ m/s) with comparison of scenario 1 (dark dashed line) and scenario 2 (light solid line). Scenarios 1 and 2 curves are nearly superimposed in both figures.

The calculated daily water exchange budget for the cavity (Fig. 5B) highlights that the water exchanges are dominated by seepage into the cavity (mean piezometric head higher that the hydraulic one in the cavity), which explains the increase of the hydraulic head in the cavity over time. This seepage presents higher values during early simulated times (more than $100 m^3$/day) and, then, it sharply decreases over the 1st week and flattens progressively around $20 m^3$/day at the end of the observation time. In terms of relative volume (Fig. 5B, right axis), the seepage represents <1% of the pumped water volume during early cycles and around 0.1% at the end of the simulation time.

As for mean drawdown, scenario 1 and scenario 2 curves are superimposed, meaning that the influence of the no-activity periods on the water daily budget in the cavity is negligible.

3.2. Influence of hydraulic conductivity of the aquifer

The influence of the hydraulic conductivity on the aquifer response is assessed by comparing the numerical results obtained by variation of K (from 1×10^{-5} to 1×10^{-9} m/s). Scenario 1 and scenario 2 are considered. The effect on the piezometric head is examined by comparing the oscillation magnitudes in the cavity and in the aquifer (Fig. 6) and a 1 week-detailed view of head evolution (Fig. 7), as well as the mean drawdown around the cavity (Fig. 8). These figures only take into account distances from the cavity up to 50 m: at further distances, computed results show weak variations. Finally, Fig. 9 shows the influence of K on computed daily seepage into the cavity.

Mean drawdown and daily seepage computed considering scenario 1 and scenario 2 are not compared because they are similar for both scenarios.

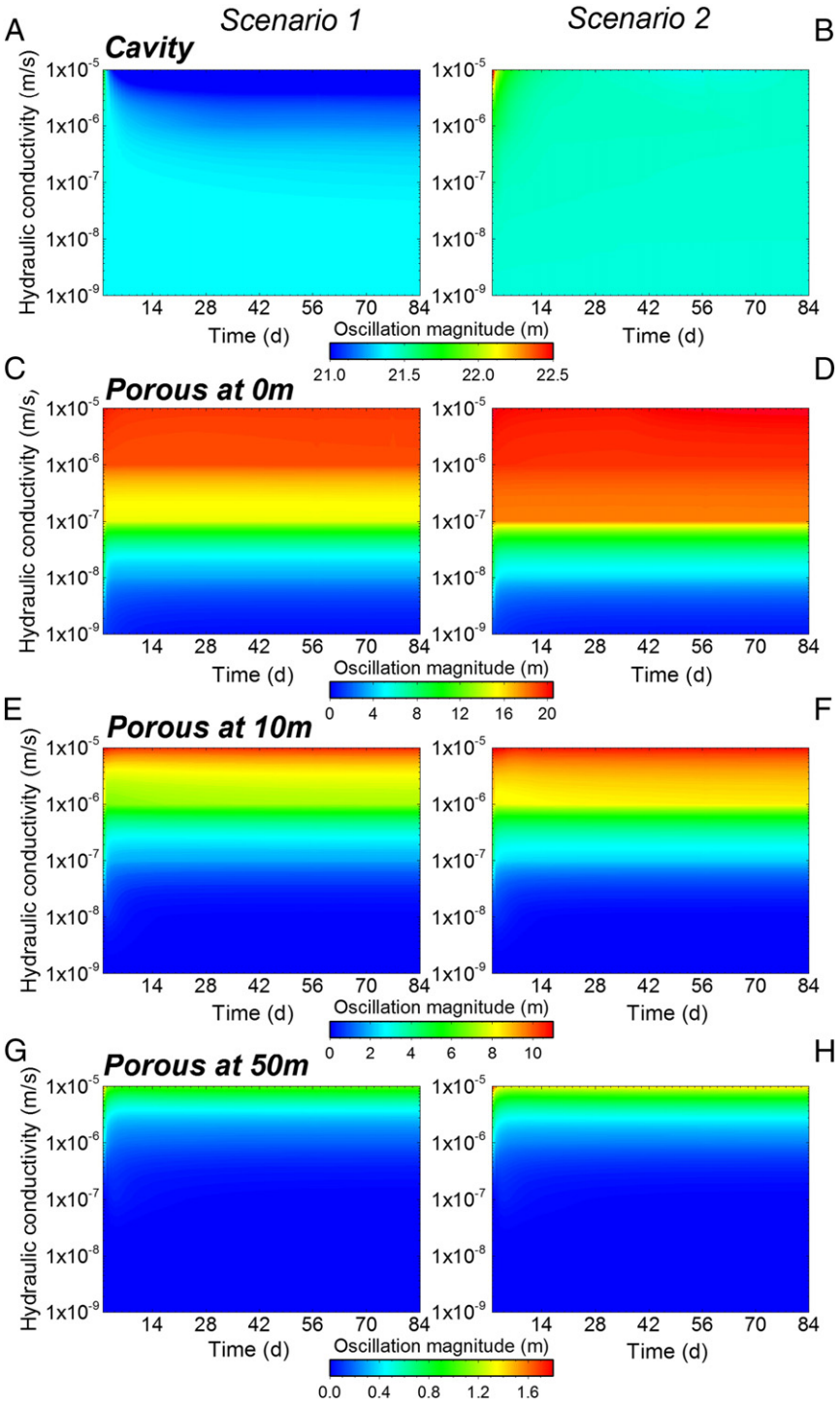

Fig. 6. Evolution of oscillation magnitude in the cavity (A–B) and in the surrounding aquifer at different distances from the cavity (C to H) for hydraulic conductivities from 1×10^{-5} m/s to 1×10^{-9} m/s: comparison of scenario 1 (left column) and scenario 2 (right column). The magnitude scale is changed for each diagram.

3.2.1. Piezometric impact

Fig. 6 shows the evolution of oscillation magnitude in the cavity and in the surrounding aquifer. The value of K influences mainly the oscillation magnitude in the surrounding aquifer: the magnitude decreases when the hydraulic conductivity is lower. In the cavity (Fig. 6A & B), the influence of the hydraulic conductivity value is quite limited, as the head variation is mainly controlled by the pumping/injection rate. However, for high hydraulic conductivities ($K > 1 \times 10^{-7}$ m/s), the oscillation magnitude is approximately 1 m smaller for scenario 2 in comparison with scenario 1, except at the early beginning. As the pumping/injection rates are not modified depending on K, the difference is produced by the variation of seepage into the cavity. Consequently, this seepage leads to increase the hydraulic head in the cavity over time, especially for higher hydraulic conductivities as it is highlighted by the shift of the piezometric head curves in comparison with lower conductivities (Fig. 7A).

In the aquifer, whatever the distance from the cavity being considered, the oscillation magnitude displays large differences between values obtained with lower and higher values of K (Fig. 6C to H). Minimum oscillation magnitudes occur for lower hydraulic conductivities.

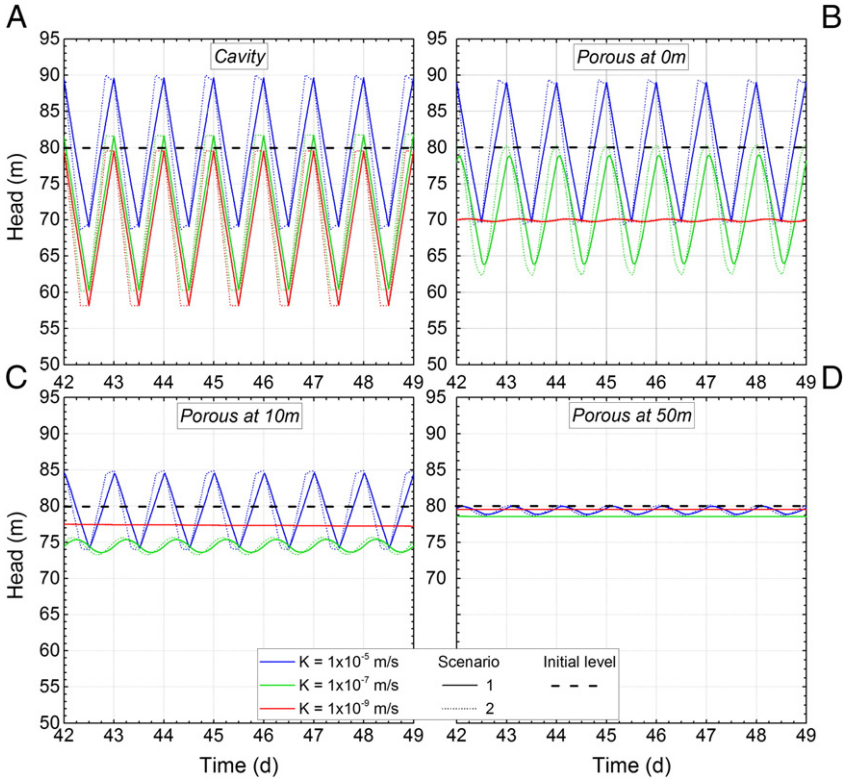

Fig. 7. Head evolution during 1 week (day 42 to day 49) in the cavity (A) and in the aquifer at different distances from the cavity (B: 0 m, C: 10 m & D: 50 m) for hydraulic conductivities from 1×10^{-5} m/s to 1×10^{-9} m/s: comparison of scenario 1 (solid line) with scenario 2 (dotted line).

This damping of magnitude for low K appears also distinctly in Fig. 7B to D with the piezometric head curves tending toward a flat line for lower K. This reflect the fact that the influence area of the pumping/injection activities is smaller for lower hydraulic conductivities.

As already pointed out in the results of the reference case, the oscillation magnitude decreases with distance from the cavity. According to the hydraulic conductivity, oscillation magnitude ranges from <1 m to 20 m near the cavity (Fig. 6C & D). Its maximum value decreases progressively with the distance and reaches up to 11 m and up to 1.7 m at respectively 10 m and 50 m from the cavity (Fig. 6E to H). The oscillations magnitude drops rapidly towards zero at further distances.

The value of the hydraulic conductivity also impacts the way the no-activity periods of scenario 2 are displayed. In the cavity, no-activity periods lead to greater oscillation magnitude (Fig. 6B): during no-activity periods, water levels keep varying, especially for $K = 1 \times 10^{-5}$ m/s (Fig.

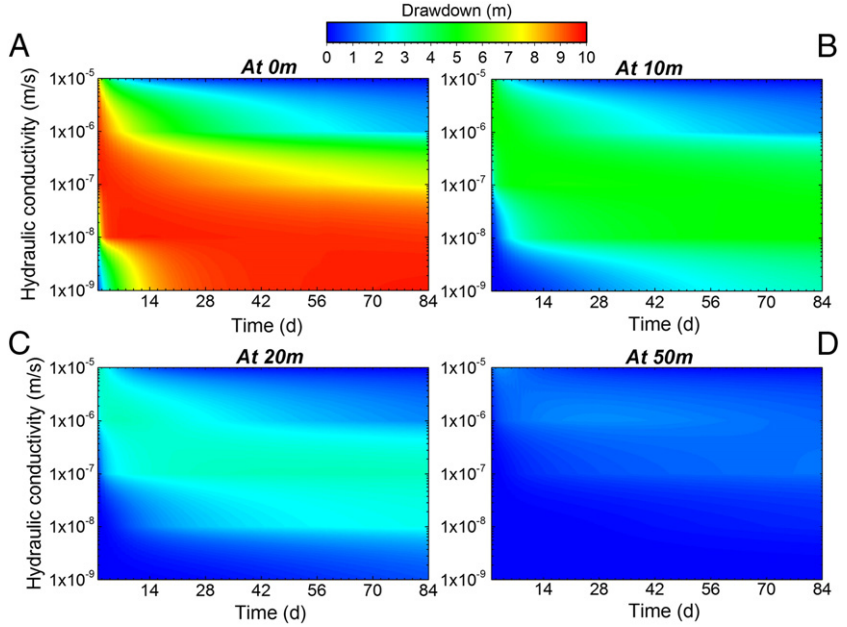

Fig. 8. Mean drawdown in the aquifer at different distances from the cavity (0 m–10 m–20 m–50 m) for hydraulic conductivities from 1×10^{-5} m/s to 1×10^{-9} m/s.

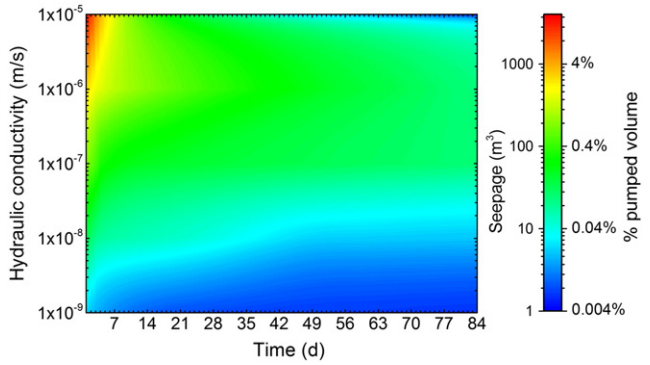

Fig. 9. Daily seepage into the cavity for hydraulic conductivities from 1×10^{-5} m/s to 1×10^{-9} m/s.

7A, dotted line). In the aquifer, the oscillation magnitude is greater for scenario 2 in case of higher hydraulic conductivities and more distinctly at smaller distance from the cavity (Fig. 6D-F-H). For these high hydraulic conductivities, the no-activity head stages in the cavity is also detected in the surrounding aquifer with progressive damping with distance from the cavity (blue dotted lines in Fig. 7B to D). In contrast, for smaller hydraulic conductivities, head stages vanish and merge with the global head oscillation (green and red dotted lines in Fig. 7B to D).

3.2.2. Influence on the mean drawdown in the surrounding aquifer

The hydraulic conductivity value modifies the influence area, the magnitude of the mean drawdown, and the evolution feature (Fig. 8). The mean drawdown is negligible at distances further than 50 m for all values of K.

The mean drawdown computed close to the cavity during early times is higher when *K* is increased (Fig. 8A & B). After the early rise, it rapidly decreases and then vanishes (i.e. calculated piezometric head oscillate finally around the initial one). On the contrary, for lower *K,* the mean drawdown increases constantly during the first weeks until reach a constant and maximum value. A significant mean drawdown takes place in the early days and then decrease slightly over time for intermediate *K*.

At further distances from the cavity (>20 m) (Fig. 8C & D), the mean drawdown evolves in the same way as previously, but with smaller magnitudes. However, for the lowest *K*, almost no mean drawdown is computed, showing that the radius of influence is limited.

3.2.3. Seepage flow rate

The cyclic pumping and injection periods create exchanges of water between the cavity and the surrounding aquifer. As already pointed out for the reference case, the daily budget of these exchanges shows that there is a net seepage into the cavity, leading to progressive increase of the cavity water level. The computed head evolution in the cavity highlights clearly this behavior, especially for higher conductivities. The hydraulic head curves in the cavity display increasing maximum values in comparison with the initial head, corresponding to the expected maximum head if no seepage occurred (Fig. 7A).

Cyclic pumping/injection periods induce seepage for every hydraulic conductivity considered (Fig. 9). For low hydraulic conductivities, seepage remains relatively constant during the whole observation time, but only with few cubic meters. It is negligible with respect the total pumped water volume per day (<0.05%) and it does not affect significantly the hydraulic head evolution. In contrast, in more permeable medium ($K > 1 \times 10^{-6}$ m/s), seepage is more important, especially during the first days of solicitation with up to 3000 m^3 of seeped water (≈12% of the daily pumped water volume). However, for these highly permeable media, the seepage is decreasing rapidly with time: after important values during the first week (over 250 m^3 equivalent to ≈1% of the daily pumped water volume), seepage drops down to 25m^3 (≈0.4% of the daily pumped water volume) and it turns to be negligible (below 10 m^3 per day) after around 30 days. Seepage decreases rapidly for highly permeable media because the mine is filled faster, and therefore, the head difference between inside and outside the cavity decrease in a short period. This behavior explains the increase of hydraulic head in the cavity and the subsequent decrease of mean drawdown: the seeped volume in the cavity allows the system recovering progressively from the initial drawdown over the observation time. For intermediate hydraulic conductivities, the seepage appears more or less stabilized and under 100m^3 (namely 0.4% of daily pumped volume).

4. Discussion

4.1. Cavity and porous medium, a reciprocal interaction

The cyclic pumpings and injections induce piezometric head oscillations in the aquifer. The magnitude of these oscillations varies according to the distance from the cavity and to the hydraulic conductivity of the aquifer. An increase of the hydraulic head in the cavity is observed at each cycle when regular cycles are considered, which leads to a rise of the mean head. This increment is produced by the net seepage from the surrounding aquifer into the underground cavity. The higher the hydraulic conductivity, the higher the seepage and, then, the higher is the total head increment in the cavity. As the mean hydraulic head increases in the cavity, the piezometric head increases also in the surrounding aquifer.

These reciprocal interactions explain the difference in the drawdown dynamic between high and low hydraulic conductivity media. For high *K*, hydraulic head increments show large values, leading to a consequent increase of mean piezometric head in the surrounding aquifer, reducing the drawdown. Consequently, the mean head in the aquifer equilibrates progressively the initial piezometric head, which remains constant at large distance from the cavity. On the other hand, in low permeable medium, seepage, and subsequent head increments, are weak, limiting the increase of mean hydraulic head in the cavity, and, therefore, in the surrounding aquifer. In addition, smaller responses to solicitations (oscillation magnitude, drawdown and influence area) are observed in this kind of aquifers, resulting in a drawdown that increases continuously or trends toward a significant constant value.

4.2. Cyclic stresses and steady state

The drawdown and seepage evolutions show both trends towards constant values over time. Head evolution, especially for high hydraulic conductivities, seem also stabilizing the oscillation around a constant value. These observations would suggest that the system could reach a "steady-state" under cyclic stresses.

For an open-pit UPSH configuration, Pujades et al. (2016) showed that cyclic pumping/injection in the cavity evolves towards a "dynamic steady-state" after the initial disruption of the system. The "dynamic steady state" is achieved when the mean head around which groundwater oscillates reaches a constant value. The time required to reach this "dynamic steady-state" appeared being dependent on the hydraulic properties of the aquifer. The higher is the hydraulic conductivity, the faster the dynamic steady-state is reached. This "dynamic steady-state" could be considered in order to explain the seepage and drawdown trends towards constant values over time. However, for most of our results, the "dynamic steady-state" is not reached. Indeed, for medium and low hydraulic conductivities, longer simulation times would be required to reach it.

4.3. Impact on feasibility

These first results point out some key features about the groundwater response under cyclic stresses created by using an old underground

mine as lower reservoir of an UPSH. These observations can be brought in a UPSH feasibility context.

Groundwater oscillations and drawdown around the cavity could either interfere with other human activities, such as pumping wells for example, either develop geomechanical instabilities in the surrounding rock environment. On the other hand, the progressive head increment in the cavity, due to the water exchanges with the surrounding aquifer, may influence the energetic efficiency. This increment depends on both the hydraulic conductivity of the porous medium and the frequency and rate of pumping cycles.

From the hydraulic conductivity sensitivity analysis, opposite outcomes for the feasibility were underlined. Low hydraulic conductivity media appeared being more suitable as the induced oscillation magnitude around the mine is lower than in high hydraulic conductivity media. Concerning the drawdown, either high or low hydraulic conductivity media could be appropriate as the drawdown tends to vanish or is very space-limited, respectively. Intermediate hydraulic conductivity media turned out to be the worst cases with a significant drawdown value, and wide area of influence. Drawdown will be negligible in case of high hydraulic conductivity media after some time because the head around groundwater oscillates reaches its initial position in a short period given the high seepage provided. Although high hydraulic conductivities are not a problem regarding the drawdown, in case of seepage, these should be avoided as the seeped water volume is clearly non-negligible and would significantly impact the efficiency with regards to additional pumping volume.

In addition to these key features, the regularity of the pumping/injection time pattern should also be considered given that the pumping/injection rate, the duration of each period and the occurrence of no-activity periods would also influence the system response. Our results show that such a system could reach at some point a “dynamic steady-state” under regular cyclic stresses, limiting therefore the impacts. However, an irregular time pattern would probably prevent reaching this kind of steady-state.

5. Conclusion

A simplified groundwater model based on a slate mine geometrical properties highlights that using an old underground cavity as lower reservoir of an UPSH will impact the surrounding aquifer. Repeated pumping/injection cycles in the underground cavity are transmitted through the aquifer as piezometric head oscillations. The magnitude of head oscillations is attenuated when reducing the hydraulic conductivity and/or considering increased distance from the cavity. Larger oscillations across a wider influence area will be expected in highly permeable porous medium. The cyclic pumping/injection solicitations also induce a mean drawdown in the surrounding aquifer with extent, magnitude, and decreasing trend dynamic depending on the hydraulic conductivity value. In low hydraulic conductive media, a significant mean drawdown is reached progressively and tends towards a constant value over time. The drawdown is however limited spatially from the cavity. In case of high permeable media, a large drawdown appears rapidly and gradually decreases over time towards a zero value. For intermediate permeable porous media, the drawdown is lower than for low hydraulic conductivity media, but it extends over a wider area.

The analysis of the water level evolution in both the aquifer and the cavity, subsequent to cyclic pumping/injection in the cavity, underlines the importance of the reciprocal interactions between the cavity and the surrounding groundwater with significant influence of hydraulic properties of the aquifer. More precisely, in addition to the piezometric head evolution in the aquifer, the solicitations also induce hydraulic head evolution in cavity as the seepage into the cavity over time, leading to an increase of the mean water level in the cavity. This process is negligible for low hydraulic conductivities but could become important for high hydraulic conductivities, influencing negatively the efficiency of an UPSH system due to additional water volume to pump.

The two different pumping/injection cycles (without and with no-activity periods), applied on our model did not significantly influence the system response (oscillation magnitude, drawdown nor seepage) because of the regularity of these cycles in terms of period duration and pumping/injection rates. It is then expected that irregular cycles of pumping/turbining, as required by realistic production/demand electricity variations, would lead to a distinctive response.

These first preliminary results highlight the main key hydrogeological features of such a project. In terms of impacts, induced head oscillations and drawdown around the cavity could have consequences on depending ecosystems or for other human activities. In terms of energetic efficiency, the progressive head increment in the cavity may influence badly the efficiency probably depending on the adopted pump and turbine characteristics. This induced head increment in the cavity depends on both the hydraulic conductivity of the porous medium and the frequency and rate of pumping cycles.

However, on future works, it will be interesting to investigate the hydrogeological feasibility in details and on a specific chosen site, with focus on the effect of non-homogeneous porous medium and of heterogeneities occurrence (e.g. fault) in the geological environment, as well as the influence on the system response of the use of realistic pumping/injection curves.

Acknowledgements

This research has been supported by the Public Service of Wallonia - Department of Energy and Sustainable Building. S. Bodeux benefits from a research grant from the FRIA (Fonds pour la Recherche dans l'Industrie et l'Agriculture, FRS-FNRS, Belgium). E. Pujades gratefully acknowledge the financial support from the University of Liège and the EU through the Marie Curie BelPD-COFUND postdoctoral fellowship (2014–2016; FP7-MSCA-COFUND, 600405).

References

Adams, R., Younger, P.L., 2001. A strategy for modeling ground water rebound in abandoned deep mine systems. Ground Water 39, 249–261.

Alvarado, R., Niemann, A., 2015. Underground pumped-storage hydroelectricity using exisiting coal mining infrastructure. 36th IAHR World Congress, pp. 1–8 (The Hague, The Netherlands).

Ardizzon, G., Cavazzini, G., Pavesi, G., 2014. A new generation of small hydro and pumped-hydro power plants: advances and future challenges. Renew. Sust. Energ. Rev. 31:746–761. http://dx.doi.org/10.1016/j.rser.2013.12.043.

Bear, J., Cheng, A.H.-D., 2010. Modeling Groundwater Flow and Contaminant Transport. Springer Science + Business Media.

Beck, H.P., Schmidt, M., 2011. Windenergiespeicherung durch Nachnutzung stillgelegter Bergwerke.

Braat, K.B., Van Lohuizne, H.P.S., De Haan, J.F., 1985. Underground Pumped Hydro-storage Project for the Netherlands. Tunnels and Tunneling 17 pp. 19–22.

Brouyère, S., 2001. Etude et Modélisation du Transport et du Piégeage des Solutés en Milieu Souterrain Variablement Saturé. University of Liège.

Brouyère, S., Carabin, G., Dassargues, A., 2004. Climate change impacts on groundwater resources: modelled deficits in a chalky aquifer, Geer basin, Belgium. Hydrogeol. J. 12:123–134. http://dx.doi.org/10.1007/s10040-003-0293-1.

Brouyère, S., Orban, P., Wildemeersch, S., Couturier, J., Gardin, N., Dassargues, A., 2009. The hybrid finite element mixing cell method: a new flexible method for modelling mine ground water problems. Mine Water Environ. 28, 102–114.

Bussar, C., Stöcker, P., Cai, Z., Moraes Jr., L., Magnor, D., Wiernes, P., van Bracht, N., Moser, A., Sauer, D.U., 2016. Large-scale integration of renewable energies and impact on storage demand in a European renewable power system of 2050 - sensitivity study. J. Energy Storage 6, 1–10.

Carabin, G., Dassargues, A., 1999. Modeling groundwater with ocean and river itneraction. Water Resour. Res. 35, 2347–2358.

Chen, H., Cong, T.N., Yang, W., Tan, C., Li, Y., Ding, Y., 2009. Progress in electrical energy storage system: a critical review. Prog. Nat. Sci. 19, 291–312.

de Haan, W.A., Min, A.P.N., 1984. Ondergrondse pomp accumulatie centrale: effectiviteitsverbetering d.m.v. verschillende pomp-turbinevermogens. TUDelft.

Deane, J.P., Ó Gallachóir, B.P., McKeogh, E.J., 2010. Techno-economic review of existing and new pumped hydro energy storage plant. Renew. Sust. Energ. Rev. 14, 1293–1302.

DGO3, 2008. Code wallon de bonnes pratiques - Gestion des sols - Guide de référence pour l'étude de risque.

Fosnacht, D.R., 2011. Pumped hydro energy storage (PHES) using abandoned mine pits on the mesabi iron range of minnesota – final report.

Ghasemizadeh, R., Hellweger, F., Butscher, C., Padilla, I., Vesper, D., Field, M., Alshawabkeh, A., 2012. Review: Groundwater flow and transport modeling of karst aquifers, with

particular reference to the North Coast Limestone aquifer system of Puerto Rico. Hydrogeol. J. 20, 1441–1461.
IEA, 2015. Energy and climate change - World Energy Outlook Special Report (doi: 10.1038/479267b).
Khan, S.Y., Davidson, I.E., 2016. Underground pumped hydroelectric energy storage in South Africa using aquifers and existing infrastructure. NEIS Conference 2016 on Sustainable Energy Supply and Energy Storage Systems (Hamburg, Germany).
Luick, H., Niemann, A., Perau, E., Schreiber, U., 2012. Coalmines as Underground Pumped Storage Power Plants (UPP) – a contribution to a sustainable energy supply? Geophys. Res. Abstr. 14, 4205.
Madlener, R., Specht, J.M., 2013. An Exploratory Economic Analysis of Underground Pumped-storage Hydro Power Plants in Abandoned Coal Mines.
Martin, G.D., 2007. Aquifer Underground Pumped Hydroelectric Energy Storage. University of Wisconsin-Madison.
Meyer, F., 2013. Storing Wind Energy Underground (Bonn, Germany).
Moriarty, P., Honnery, D., 2016. Can renewable energy power the future? Energy Policy 93:3–7. http://dx.doi.org/10.1016/j.enpol.2016.02.051.
Niemann, A., 2011. Machbarkeitsstudie zur Nutzung von Anlagen des Steinkohlebergbaus als Pumpspeicherwerke. Pumpspeicherkraftwerke Unter Tage: Chance Für Das Ruhrgebiet (Essen, Germany).
Poulain, A., Goderniaux, P., De Dreuzy, J.-R., 2016. Study of groundwater-quarry interactions in the context of energy storage systems. European Geosciences Union General Assembly - Geophysical Research Abstracts, p. 18 (Vienna, Austria).
Pujades, E., Willems, T., Bodeux, S., Orban, P., Dassargues, A., 2016. Underground pumped storage hydroelectricity using abandoned works (deep mines or open pits) and the impact on groundwater flow. Hydrogeol. J.:1–16 http://dx.doi.org/10.1007/s10040-016-1413-z.
Rapantová, N., Grmela, A., Vojtek, D., Halir, J., Michalek, B., 2007. Groundwater flow modelling applications in mining hydrogeology. Mine Water Environ. 26, 264–270.
Rehman, S., Al-Hadhrami, L.M., Alam, M.M., 2015. Pumped hydro energy storage system: a technological review. Renew. Sust. Energ. Rev. 44:586–598. http://dx.doi.org/10.1016/j.rser.2014.12.040.
Severson, M.J., 2011. Preliminary evaluation of establishing an underground Taconite Mine, to be used later as a lower reservoir in a pumped hydro energy storage facility, on the Mesabi Iron Range, Minnesota.
Sherwood, B.M., Younger, P.L., 1994. Modelling groundwater rebound after coalfield closure: an example from County Durham , UK. 5th International Mine Water Congress, pp. 769–777 (Nottingham, UK).
Spriet, J., 2013. A feasibility study of pumped hydropower energy storage systems in underground cavities. Bruface (ULB - VUB Faculty of Engineering).
Steffen, B., 2012. Prospects for pumped-hydro storage in Germany. Energy Policy 45, 420–429.
Surinaidu, L., Gurunadha Rao, V.V.S., Srinivasa Rao, N., Srinu, S., 2014. Hydrogeological and groundwater modeling studies to estimate the groundwater inflows into the coal Mines at different mine development stages using MODFLOW, Andhra Pradesh, India. Water Resour. Ind. 7–8, 49–65.
Tam, S.W., Blomquiot, C.A., Kartsounes, G.T., 1978. Underground Pumped Hydro Storage - An Overview (Ardonne, Illinois).
Wildemeersch, S., Brouyère, S., Orban, P., Couturier, J., Dingelstadt, C., Veschkens, M., Dassargues, A., 2010. Application of the Hybrid Finite Element Mixing Cell method to an abandoned coalfield in Belgium. J. Hydrol. 392, 188–200.
Wong, I.H., 1996. An underground pumped storage scheme in the Bukit Timah granite of Singapore. Tunn. Undergr. Space Technol. 11, 485–489.
Yeh, G.T., 1987. 3DFEMWATER: a 3-dimensional finite element model of WATER flow through saturated-unsaturated media. ORNL-6386, Oak Ridge National Laboratory, Oak Ridge, Tenessee.
Yekini Suberu, M., Wazir Mustafa, M., Bashir, N., 2014. Energy storage systems for renewable energy power sector integration and mitigation of intermittency. Renew. Sust. Energ. Rev. 35:499–514. http://dx.doi.org/10.1016/j.rser.2014.04.009.